

# Catalytic Upgrading of the Hydrothermal Liquefaction Aqueous Phase Using Zeolites

## **A Major Qualifying Project**

Submitted to the Faculty of Worcester Polytechnic Institute  
In partial fulfillment of the requirements for the degree in  
Bachelor's of Science in Chemical Engineering

### **Submitted by**

Alex Mosley  
Oamfah (Faith) Suwannapong  
Jia Yazon

### **Submitted on**

April 25, 2024

### **Project Advisor**

Michael Timko

*This report represents the work of WPI undergraduate students submitted to the faculty as evidence of a degree requirement. WPI routinely publishes these reports on its website without editorial or peer review. For more information about the projects program at WPI, see <http://www.wpi.edu/Academics/Projects>.*



# WPI

## **ACKNOWLEDGEMENTS**

First, we would like to thank BASF for supplying the ZSM-5 catalyst throughout the experiment period. This project would not have been possible without the help of several WPI faculty and staff in the Chemical Engineering Department. We would like to thank Assistant Research Professor, Alex Maag for performing TEA analysis and providing project guidance when we faced difficulties during the experiments.

We would also like to thank Assistant Research Professor, Geoffrey Tompsett for his assistance with project guidance and X-ray diffraction and Raman Spectroscopy used to characterize the catalyst.

We would also like to thank Skyler Kauffman for writing TOC analysis instructions and supporting us during the experiments. We would also like to thank Lab Manager and Advanced Machinist, Ian Anderson, and Electronics Engineer, Douglas White for their assistance in repairing and redesigning the reactor.

Finally, we also want to thank our advisor, Professor of Chemical Engineering, Michael Timko, for his extensive knowledge, generous support, and advice for research direction and our future career paths.

## ABSTRACT

Biofuels are a growing sector of renewable energy that can contribute to sustainable progress. However, one biofuel-making process, Hydrothermal Liquefaction (HTL), creates a toxic and costly aqueous phase byproduct (HTL-AP). The HTL-AP has high levels of organic content and nitrogenous compounds, which requires expensive wastewater treatment. This project explores an opportunity to treat and extract value from the HTL-AP through a post-HTL process called HTL-AP Upgrading (HTL-APU). This process uses ZSM-5 in a continuous, packed-bed reactor. ZSM-5 has proven effective at cracking reactions and aromatic formation, making it a feasible option for HTL-APU. Performance of ZSM-5 on organic removal and aromatic production was studied at supercritical water conditions, with temperatures ranging from 380 to 440 °C, and pressure at 3500 PSI. Overall, yield was shown to increase with higher temperatures, with a local maximum achieved at 420 °C with 88% total organic content removal. However, ZSM-5 showed increased degradation at higher temperatures, resulting in a decreased yield above 420 °C. The high production of aromatics throughout the experiment indicates potential for bio-crude production, and the removal of nitrogen compounds from the HTL-AP indicates denitrogenation chemistry. Future research opportunities lie in studying stabilized versions of ZSM-5, and in defining the turning point where catalyst degradation overtakes increased chemical activity at higher temperatures.

**Key Words:** Hydrothermal Liquefaction, Aqueous Phase, Zeolite Catalysis, ZSM-5, Aqueous Phase Valorization, Catalytic Upgrading, Catalytic Reactor, Supercritical Water, Techno-Economic Analysis

## TABLE OF CONTENTS

<b>1. INTRODUCTION.....</b>	<b>1</b>
<b>2. BACKGROUND.....</b>	<b>2</b>
2.1 Hydrothermal Liquefaction and the Aqueous Phase Byproduct.....	2
2.2 Valorization of the HTL Aqueous Phase.....	3
2.3 Prior Research in ZSM-5 Activity and HTL-APU.....	4
<b>3. METHODS.....</b>	<b>5</b>
3.1 Materials.....	5
3.2 Continuous Flow Reactor Design and Operation.....	5
3.2.1 Design and Setup.....	5
3.2.2 Sample Collection for HTL-APU.....	6
3.2.3 Reactor Maintenance During Operation.....	6
3.4 Material Characterization.....	6
3.5 Techno-Economic Analysis.....	7
<b>4. RESULTS &amp; DISCUSSION.....</b>	<b>9</b>
4.1 Preliminary Material Characterization.....	9
4.2 Post-Reaction HTL-AP Characterization.....	10
4.3 Catalyst Stability.....	13
4.4 Techno-Economic Analysis.....	15
<b>5. CONCLUSION.....</b>	<b>17</b>
<b>6. FUTURE WORK &amp; RECOMMENDATIONS.....</b>	<b>17</b>
<b>References.....</b>	<b>19</b>
<b>Appendices.....</b>	<b>24</b>

## LIST OF TABLES

<b>Table 1:</b> HTL-APU yield at varying temperatures.....	11
<b>Table 2:</b> Experimental Data from HTL-APU run at 380 °C.....	27
<b>Table 3:</b> Experimental Data from HTL-APU run at 400 °C.....	27
<b>Table 4:</b> Experimental Data from HTL-APU run at 420 °C.....	28
<b>Table 5:</b> Experimental Data from HTL-APU run at 440 °C.....	28

## LIST OF FIGURES

<b>Figure 1:</b> PFD of the Continuous Flow Reactor.....	5
<b>Figure 2:</b> HTL process with HTL-APU diagram (Snowden-Swan et al., 2016).....	7
<b>Figure 3:</b> GC-MS analysis of HTL-AP and centrifuged HTL-AP.....	9
<b>Figure 4:</b> X-Ray Diffraction (XDR) analysis of ZSM-5.....	10
<b>Figure 5:</b> Pictures of HTL-AP samples before and after reacting at varying temperatures.....	10
<b>Figure 6:</b> Total organic content of reacted HTL-AP samples at varying temperatures.....	11
<b>Figure 7:</b> Gas chromatography and mass spectroscopy data of aromatic compounds at varying temperatures.....	12
<b>Figure 8:</b> Gas chromatography and mass spectroscopy data of nitrogen-containing compounds at varying temperatures.....	13
<b>Figure 9:</b> Photos of ZSM-5 before and after use in the reactor.....	14
<b>Figure 10:</b> X-Ray Diffraction graph of ZSM-5 before and after use at different temperatures....	14
<b>Figure 11:</b> Gas chromatography and mass spectroscopy data of aromatic compounds at different times throughout a trial at 400 °C.....	15
<b>Figure 12:</b> Result of the techno-economic analysis showing bio-crude selling price and the required APU yield to offset its cost.....	16
<b>Figure 13:</b> Raman Spectroscopy analysis of ZSM-5 as prepared and calcined ZSM-5.....	25
<b>Figure 14:</b> Example of raw GC/MS data.....	25
<b>Figure 15:</b> Table created by using the SUMIF function to analyze GC/MS data.....	26
<b>Figure 16:</b> Screenshot of compounds name and peak areas, obtained from GC/MS) in treated HTL-AP at 380 °C & 1.5h.....	29
<b>Figure 17:</b> Example of TOC return sheet.....	30

# 1. INTRODUCTION

Biofuels are an emerging sector of clean energy and a potential solution for the transition to sustainable energy. A growing technology in biofuel production is the Hydrothermal Liquefaction (HTL) process. However, HTL creates a toxic aqueous phase byproduct (HTL-AP) that is contaminated with high concentrations of organics and nitrogenous compounds. The presence of these chemicals can create an imbalance in aquatic ecosystems if released to the environment without treatment. Therefore, the HTL-AP is often sent to external wastewater treatment plants. This step is particularly expensive, contributing to the high cost of biofuels and HTL biocrude especially. Additionally, the carbon-rich HTL-AP stream is often treated as a wastewater stream, but is actually an opportunity to further extract more biocrude for a greater yield in the entire HTL system. Thus, the goal of this project was to investigate an alternative process to remove the organics in the HTL-AP: catalytic upgrading.

Most catalysts cannot withstand the corrosive properties of the HTL-AP (Han et al., 2016). However, ZSM-5, a zeolite catalyst, has much higher chemical and thermal stability (Li et al., 2020). These characteristics coupled with ZSM-5's favorability toward cracking and denitrogenation reactions in bio-oil make it an especially promising candidate for HTL-APU (Duan et al., 2013). However, there are limitations to the operating conditions of this catalyst. For example, the catalyst has been shown to degrade in hot liquid water conditions (Maag et al., 2019). Additionally, most research on ZSM-5 has been done with batch processes rather than continuous (Duan et al., 2013; Han et al., 2016; Li et al., 2020; Maag et al., 2019).

Catalytic upgrading of the HTL-AP with ZSM-5 in a continuous reactor process has not yet been studied. Therefore, we aimed to address this gap by investigating ZSM-5 performance on organic removal in the HTL-AP at different temperatures while maintaining supercritical conditions. ZSM-5 performance was assessed through characterization of the HTL-AP and ZSM-5 before and after the reaction process.

To conduct an analysis on ZSM-5 performance in a continuous flow reactor, a packed-bed reactor was assembled. Operating conditions were controlled using insulation and a heater, as well as a back pressure regulator to maintain supercritical conditions. Using this system, the reaction was conducted at temperatures ranging from 380 °C to 440 °C for 3 hours with a space velocity of 7.7 hr<sup>-1</sup>. Samples were collected at 30-minute intervals, then characterized using gas chromatography/mass spectroscopy. Additionally, ZSM-5 was assessed using X-ray diffraction. Finally, the economic implications of this process were projected using a techno-economic analysis. These results provide more insight into ZSM-5 and the opportunities that the HTL-AP stream poses for development in clean energy.

## 2. BACKGROUND

The current climate crisis is a consequence of human-made processes that promote the production of carbon dioxide in Earth's atmosphere. Dependence on fossil fuels, a limited resource, particularly contributes to the global warming phenomenon (LeClerc et al., 2023). Additionally, issues of poor waste management contribute to the further release of greenhouse gases into the environment (Onyanta, 2016). To combat the dangerous effects of higher carbon dioxide levels, efforts are being made to transition energy dependence to renewable and clean energy sources, such as hydropower, geothermal, and wind (Dincer, 2000). One particular form of renewable energy, biofuels, is currently a promising, yet under-developed, topic of study (LeClerc et al., 2023). This emerging technology is especially promising as it addresses waste management while supplying an alternate energy source by converting biomass (including waste) into fuel. An emerging process for producing biofuels is Hydrothermal Liquefaction, or HTL (Biller et al., 2016).

### 2.1 Hydrothermal Liquefaction and the Aqueous Phase Byproduct

Hydrothermal Liquefaction (HTL), also referred to as hydrous pyrolysis, of wet biomass has proven to be a promising method for producing bio-crude oil. HTL is conducted at high temperature and pressure in an oxygen-deprived enclosure for enough time to allow for the thermochemical conversion pathway to take place (Gollakota et al., 2018). Typical operating conditions for HTL are between 250-400 °C and 4-22 MPa with residence times of 10-60 minutes (Valdez et al., 2012). At these conditions, organic feedstocks like food waste, woody biomass, algae, and sewage sludge in a subcritical or supercritical water reaction medium that enhances mass transfer produce a product mixture containing a carbon-rich bio-oil phase, an aqueous byproduct phase, and solid and gas residue (Tian et al., 2014; Wu et al., 2017). The immediate bio-crude product of HTL does not meet current fuel standards, but can be upgraded through a range of techniques to produce a useful product that competes with nonrenewable fuels (Ramirez et al., 2015). Because biomass feedstocks have diverse compositions, including carbohydrates, lignin, proteins, and lipids, the reaction chemistry and mechanisms associated with biomass liquefaction are complex (McKendry, 2002). Although the exact reaction mechanism remains largely unreported in the literature, the basic pathway can be broken into three steps: depolymerization of the biomass, decomposition of biomass monomers by cleavage; dehydration, decarboxylation and deamination; and recombination and repolymerization of reactive fragments (Demirbas, 2000).

When compared with other biomass conversion technologies, HTL stands out for its versatility in handling diverse feedstocks and producing a higher-quality liquid bio-oil (Gollakota et al., 2018).

Another strength is its unique capability to process wet feedstocks due to the fact that water is an important reactant and catalyst in the process, whereas many other processes require an energy-consuming drying step to work effectively (Toor et al., 2011). Additionally, HTL's high temperature and pressure operating conditions remain less drastic than technologies like gasification or methanation (Ocampo et al., 2023). These aspects contribute to simplifying the overall HTL process, increasing its viability and competitiveness with other processes.

A main disadvantage of the HTL process, however, is its toxic aqueous-phase byproduct (HTL-AP). HTL-AP shows high levels of organic pollution as well as high biological toxicity for traditional test organisms (Kulikova et al., 2023). Many researchers believe that, in order to ensure environmental safety and economic feasibility, HTL-AP must be valorized in some way (SundarRajan et al., 2021). Previously attempted valorization methods include HTL recycling, algae cultivation, extraction of value-added chemicals, and methanation (Swetha et al., 2021).

## **2.2 Valorization of the HTL Aqueous Phase**

There are many different processes used for HTL-AP valorization, including HTL recycling, algae cultivation, extraction of value-added chemicals, and methanation. HTL recycling loops the byproduct aqueous phase through the process, which has the effect of improving HTL yield while simultaneously lowering the total volume of aqueous phase leaving the process (Biller et al., 2016). SundarRajan et al. (2021) describes another process, called algae cultivation, which treats the wastewater with an adsorbent, after which the wastewater is used in cultivating microalgae for further bio-fuel processing. Another possible method is methanation, which produces bio-methane from the HTL-AP through other processes, such as anaerobic digestion (Watson et al., 2020). One other method is extracting value-added chemicals, in which useful chemicals are extracted from the HTL-AP, such as glycolic acid—an in-demand chemical for cosmetics (Swetha et al., 2021). Each of these processes improve the HTL process in different ways by adding more value to the aqueous phase byproduct, and more processes continue to arise as the technology develops.

One arising method for HTL-AP valorization is to use zeolites as a catalyst. The zeolite catalyst essentially breaks the C-C bonds within the contaminating hydrocarbons in the HTL-AP, lowering the total COD and the stream's toxicity (Swetha et al., 2021). This effect even adds a financial benefit by possibly eliminating the need to send the wastewater to a treatment plant. Although valorization processes are advantageous overall, there is limited research or literature on HTL-AP valorization. Therefore, this study provides a deeper analysis on the use of a zeolite-based catalyst in order to upgrade the aqueous phase derived from HTL.

### 2.3 Prior Research in ZSM-5 Activity and HTL-APU

Due to the presence of a high amount of carbon content and toxicity in the HTL-AP, its direct application as wastewater is hindered. In order to obtain high-quality HTL-AP and overcome the existing drawback of the HTL process, heterogeneous catalytic upgrading is a promising process. Heterogeneous catalysis, in this process, is a cycle of molecular reactions occurring at a solid acid catalyst surface. Critical factors affecting the catalyst activity and selectivity are the acid sites, pore sites, surface area, and water tolerance. Many heterogeneous catalytic reactions have been accomplished in gas and organic solvent phases. However, most catalysts cannot fully activate their catalytic ability in the aqueous phase due to the rapid deactivation from corrosive protons, hydroxides, or dissolved organic in water (Han et al., 2016).

Among heterogeneous catalysts, ZSM-5 zeolite is a good prospect for HTL-APU development. ZSM-5, an industrially important catalyst, is a highly siliceous crystalline aluminosilicate with abundant acid sites, special pore structure, and high thermal and chemical stability (Li et al., 2020). The Bronsted acid sites (BAS) in ZSM-5, also known as bridging OH-H groups, are formed when an oxygen atom between Si and Al tetrahedral centers is protonated to balance charges. These acid sites can further promote hydride transfer and cyclization reaction which is sufficient for formation of short-chain alkanes and aromatics from the upgrading of fatty acids and bio-oil (Ji et al., 2017). In particular, at a catalytic upgrading process at 240 °C and 6 MPa for 240 minutes, ZSM-5 can enhance cracking reaction of pretreated algae bio-oil with high activities towards denitrogenation, deoxygenation, and desulfurization (Duan et al., 2013). Also, Li & Savage (2013) report a large composition of hydrocarbon molecules in treated algae bio-oil after the catalytic upgrading with ZSM-5 at 4.35 MPa for 4 hours with higher yield of aromatic hydrocarbons at the operation temperature above 400 °C and exclusively almost aromatic hydrocarbon at 500 °C.

One challenge of this upgrading, however, is the catalyst's short deactivation due to the simple microporous structure and long diffusion pathway. Many approaches have been done to improve ZSM-5 stability and its aromatic selectivity such as structural modification of catalyst pores, ratio adjustment of Si/Al, and doping catalyst with active parts such as Fe, Co, Ni, and Zn (Kariim et al., 2023). One promising approach is to operate the catalytic reaction in the presence of supercritical water. Compared to other zeolites, ZSM-5 is found to enhance dodecane cracking and benzene, toluene, ethylbenzene, and xylene (BTEX) formation in the experiments performed over 15 wt% or less water loading at 400 °C and 25 MPa (Zaker et al., 2022). These experiments at supercritical water conditions also result in a one-phase oil-water condition which can decrease coke precursor formation and, thus, is an optimal condition for catalyst stability. To date, the main focus of upgrading experiments with ZSM-5 has been operated at supercritical water conditions in batch processes (Kariim et al., 2023; Zaker et al., 2022).

## 3. METHODS

The following sections describe the techniques and materials used throughout this research.

### 3.1 Materials

The HTL-AP used in this study is an aqueous byproduct of hydrothermal liquefaction obtained from Pacific Northwest National Laboratory's continuous flow sewage sludge HTL system. Characterization of our feed indicated a high total organic content of 18,000 PPM, with many nitrogenous organic compounds present. To prevent plugging, the feedstock was cold-centrifuged at  $-5\text{ }^{\circ}\text{C}$  for 3 hours at 3000 RPM, separating 1-2 wt% of its heaviest organic compounds.

The catalyst used for the experiment was provided from BASF Catalysts: a 40% ZSM-5 zeolite silica bound powder, with 96-104  $\mu\text{m}$  size. A calcination procedure is required to activate ZSM-5 active sites and remove organic residue from synthesis before use. ZSM-5 has been shown to be sensitive to water, including air moisture (Wu et al., 2016). Therefore, the catalyst powder was heated to  $100\text{ }^{\circ}\text{C}$  for 1 hour prior to calcination at  $550\text{ }^{\circ}\text{C}$  for at least 16 hours at ambient pressure.

### 3.2 Continuous Flow Reactor Design and Operation

#### 3.2.1 Design and Setup

The continuous flow reactor design is shown in Figure 1.

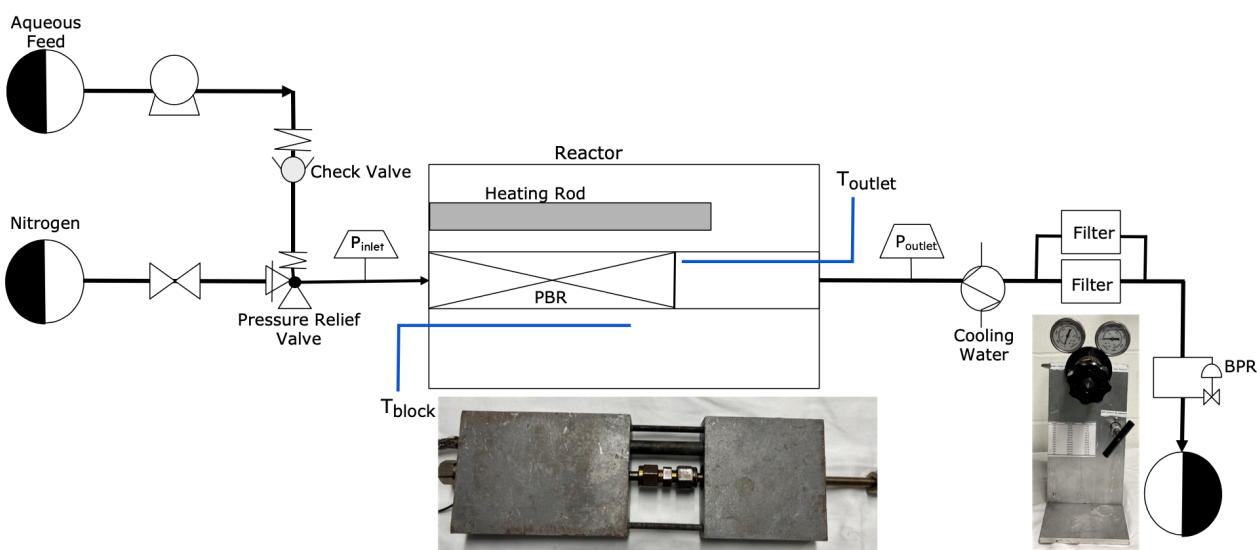


**Figure 1.** PFD of the Continuous Flow Reactor

The reactor was first packed with the catalyst powder. Then, the system was pressurized to at least 3200 PSI (typically 3500 PSI) using nitrogen gas. Nitrogen gas was used to prevent exposure of the zeolite catalyst to moisture in the air. The pressurized system was then set to the desired inlet temperature (380-440°C). Due to the limitations of the reactor block and surrounding insulation, it was required to define the setpoint temperature around 100 °C higher than the desired operating temperature of the trial. The actual reactor bed temperature was read through a separate thermocouple within the reactor.

Once the system reached the setpoint temperature, HTL-AP was pumped through the system at a flow rate of 0.25 ml/min (or a space velocity of 7.7 hr<sup>-1</sup>), thus allowing the system temperature to drop and settle at the desired operating temperature for the catalytic upgrading process. If the temperature fluctuated or did not reach the desired operating temperature, the heater setpoint was manually controlled until the system reached steady-state at the target bed temperature.

### 3.2.2 Sample Collection for HTL-APU

Once supercritical water conditions were reached within the reactor and temperature remained steady, the system was considered to be at steady-state and sample collection began. Samples were collected in vials, which were placed under the system outlet. Samples were collected every 30 minutes for 3 total hours. After 3 hours, the feed flow was stopped. The reactor was depressurized once the outlet temperature reached below 70 °C. More nitrogen gas was used to purge the reactor from excess HTL-AP in the reactor before disassembling the system to clean it.

### 3.2.3 Reactor Maintenance During Operation

A wide variety of difficulties arose during reactor operation, requiring maintenance during runs for the trial to go smoothly. One issue that required monitoring throughout the experiment was inlet and outlet pressure. A pressure too high at the inlet risked damaging the pump and indicated plugging within the reactor bed. Additionally, plugging could be indicated by a pressure drop greater than usual (~200 PSI) across the bed. Another issue that sometimes appeared in operation was bubbling within the HTL-AP feed tube. This required purging the bubbles through the pump bypass using a siphon, as gas entering the pump may cause damage. Another issue with operating at these conditions was the integrity of the reactor itself. This was maintained by leak checking and replacing parts or fittings between runs. Recommendations based on these issues are explained further in section 6.

## 3.4 Material Characterization

Performance was assessed through characterization methods for both the liquid HTL-AP samples, and the ZSM-5 catalyst. Samples of each material were analyzed before and after

preparation (cold centrifuge and calcination, respectively). Then, samples of each material were analyzed after the HTL-APU process to see the effect of the reaction.

The HTL-AP samples were analyzed using Gas Chromatography and Mass Spectrometry, or GC/MS and Total Organic Content, or TOC, analysis. For GC/MS, samples were extracted using a 1:1 volume ratio with dichloromethane (DCM). The GC/MS data was then used to observe trends in the presence of aromatic compounds and nitrogenous compounds using 1  $\mu\text{L}$  injections. The data was analyzed using a slope of peak integration of 500 for all total ion chromatograms (TICs). For TOC, samples were diluted by a factor of  $1.5 \times 10^{-4}$ . The TOC data was then used to calculate yield, or TOC removal, in each sample. To characterize ZSM-5, X-ray diffraction (XRD) was used.

### 3.5 Techno-Economic Analysis

A Techno-Economic Analysis (TEA) was used to estimate the economic impacts of adding the HTL-APU unit onto an existing bio-crude production process with HTL. The TEA model used for this analysis is based on a 2016 Pacific Northwest National Laboratory (PNNL) report (Snowden-Swan et al., 2016). The PNNL report sends the HTL-AP to a catalytic hydrothermal gasification unit, as shown by stream 132 in Figure 2. However, the TEA used for HTL-APU substitutes the CHG HTL-AP treatment with HTL-APU.

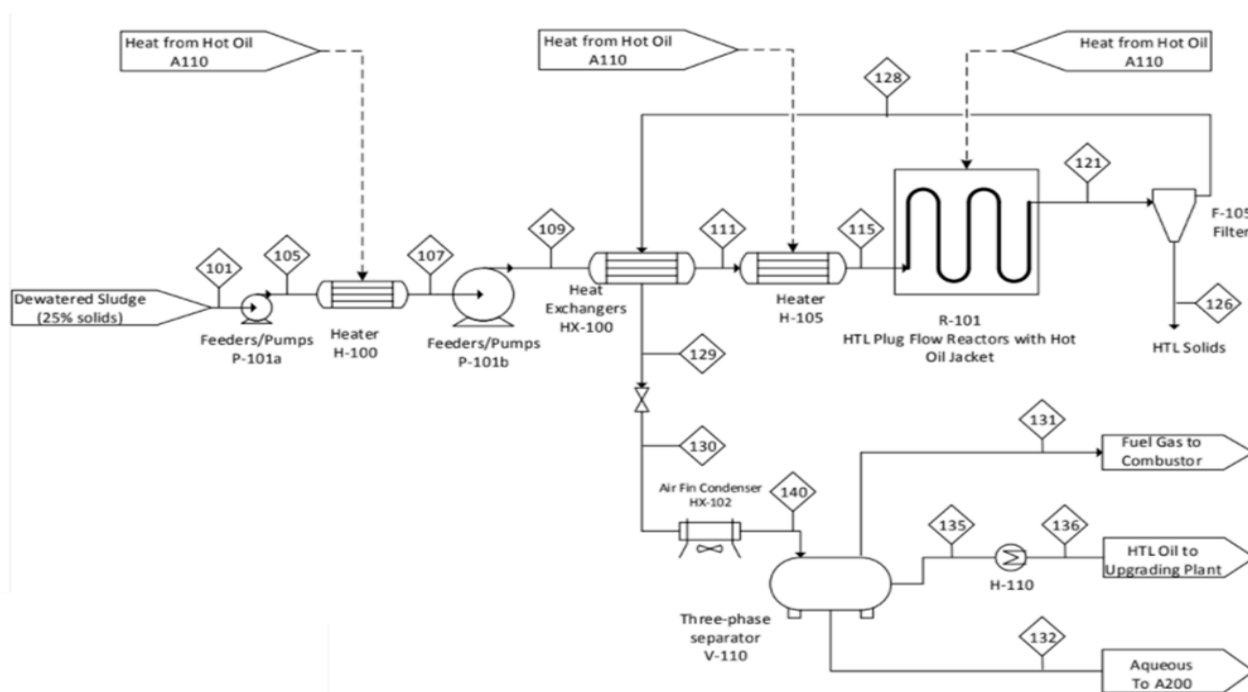


**Figure 2.** HTL process with HTL-APU diagram (Snowden-Swan et al., 2016)

The TEA model, performed in Excel, was altered from the 2016 PNNL report by adding the capital and operating costs required for the HTL-APU reactor. The cost to purchase the catalyst was relatively small and assumed to be \$0 in the calculation.

Prior to entering the HTL-APU system, the chemical oxygen demand (COD) of HTL-AP (stream 132 on Figure 2) was calculated using experimental TOC data. After the HTL-APU, treated HTL-AP was sent to an additional operation to extract rich aromatics compounds and combine them with biocrude oil produced from the HTL process to enhance overall biocrude oil production.

A discounted cash flow rate of return (DCFROR) method was applied to determine the bio-crude selling price required for a process net present value of \$0 over 30 years. Implementing HTL-APU in biocrude oil production requires additional capital and operating costs, yet this process enhances biocrude oil production and could further decrease the biocrude oil selling price.

## 4. RESULTS & DISCUSSION

### 4.1 Preliminary Material Characterization

To prepare for the experiment, the HTL-AP was cold-centrifuged and the ZSM-5 was calcined. To observe whether these preparation steps altered the chemistry of the HTL-AP and structure of the ZSM-5, samples of each were characterized before and after their respective preparation.

First, Gas Chromatography and Mass Spectrometry (GC/MS) were used to analyze the HTL-AP. Figure 3 shows representative GC/MS data of HTL-AP and cold-centrifuged HTL-AP. The organic compounds are mostly pyrazines and pyrrolidinone, as shown on the peaks at 7.5 and 17 minutes respectively. Each compound peak is located on the same retention time with fewer peak areas in centrifuged HTL-AP, indicating a lower concentration of each compound in the HTL-AP, but no change in the chemistry of these HTL-AP post-cold centrifuge. This change in concentration could be due to the small error of sample concentration injected onto the GC/MS column.

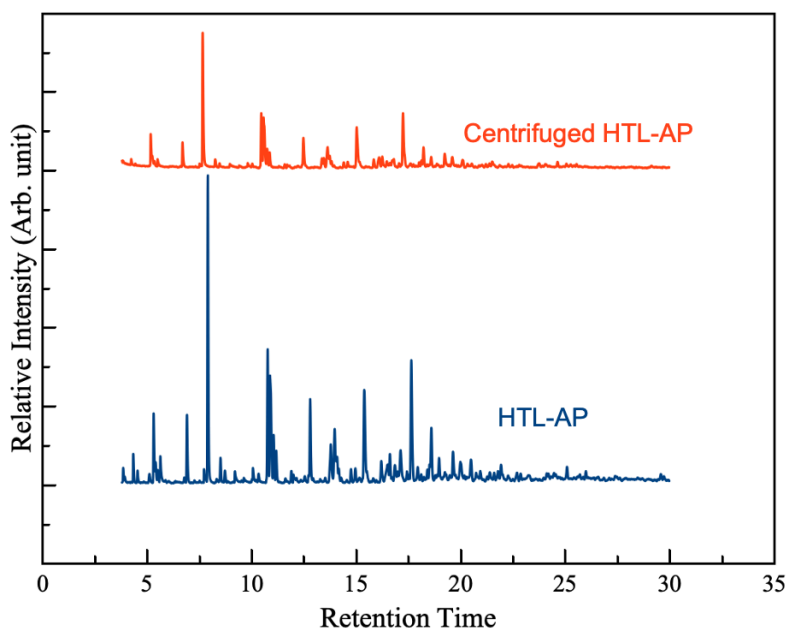


**Figure 3.** GC-MS analysis of HTL-AP and centrifuged HTL-AP

Similarly, ZSM-5 was analyzed using X-ray diffraction (XRD) and Raman Spectroscopy before and after calcination. From Figure 4, the XRD results show that the catalyst consists predominantly of ZSM-5, alumina, and amorphous Silica. The peaks of the catalyst before and after calcination are located at the same degree ( $2\theta$ ) location suggesting no change in chemical composition and crystallization of the catalyst after the calcination. The Raman

Spectroscopy analysis, shown in Appendix B.1, also shows evidence of the same catalyst composition pre and post calcination.

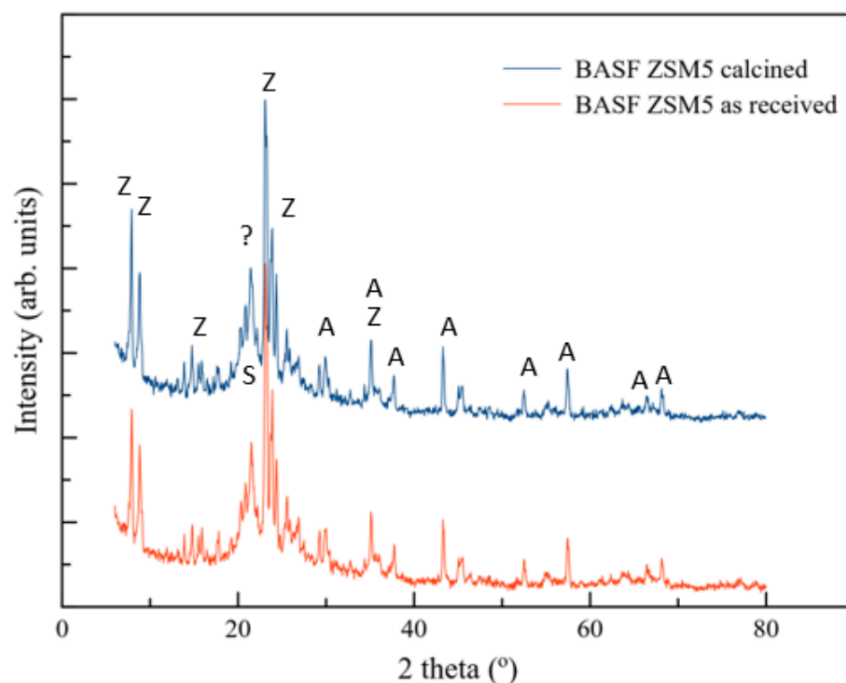


**Figure 4.** X-Ray Diffraction (XDR) analysis of ZSM-5 as prepared and calcined ZSM-5 where Z: ZSM-5, A: Alumina, and S: Amorphous Silica

#### 4.2 Post-Reaction HTL-AP Characterization

Next, the collected HTL-AP samples at each temperature were characterized using TOC and GC/MS. Visually, the samples showed a significant change in turbidity and color post-reaction. There was a slight difference in color between the samples collected at different temperatures, as shown in Figure 5.



**Figure 5.** Pictures of HTL-AP samples before and after reacting at varying temperatures. From left to right: Unreacted HTL-AP, 380 °C, 400 °C, 420 °C, 440 °C.

There were also trends in TOC levels across the different temperatures, with a local minimum at 420 °C as shown in Figure 6. From these TOC levels, the average removal yield at each temperature was also calculated, where yield is the percent of TOC removed from the unreacted HTL-AP, as displayed in Table 1. Overall, TOC showed optimal TOC removal at 420 °C with an 88% HTL-APU yield.

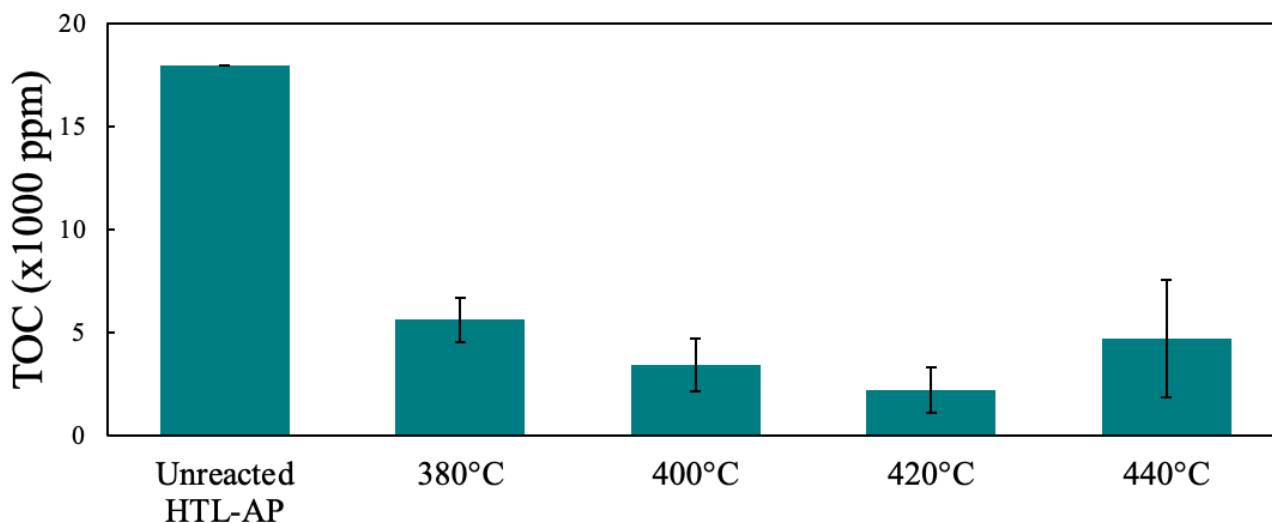


**Figure 6.** Total organic content of reacted HTL-AP samples at varying temperatures

**Table 1.** HTL-APU yield at varying temperatures

HTL-AP	HTL-APU Yield (%)
Pre-treated	-
380 °C	69 ± 6
400 °C	81 ± 7
420 °C	88 ± 6
440 °C	74 ± 16

The GC/MS data displayed in Figure 7 reveals more information regarding this trend of reactivity across different temperatures. First, the GC/MS showed a change in chemical composition within the HTL-AP. While there was an overall decrease in organic content in each treated HTL-AP sample, there was an increase in carbon aromatics, changing from 1.89% peak area to over 50% peak area in the GC/MS curve. This increase indicates that the catalyst is producing these aromatic compounds, which may have implications for further bio-crude production. These compounds are valuable components of bio-crude due to their high energy

density, which suggests that the treated HTL-AP samples contain precursors that can be converted into bio-crude.

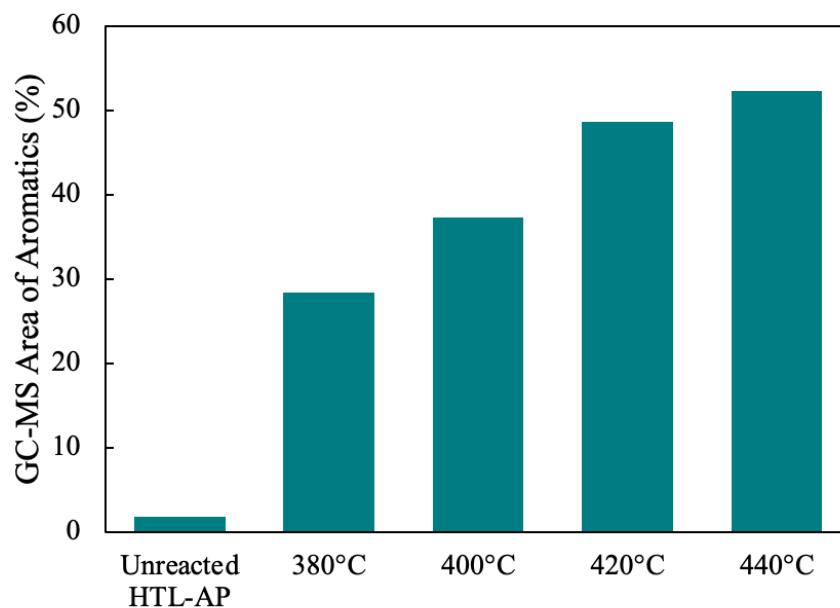


**Figure 7.** Gas chromatography and mass spectroscopy data of aromatic compounds at varying temperatures

Additionally, the data suggests denitrogenation chemistry occurring throughout the HTL-APU process as well. As shown in Figure 8, the total number of nitrogen-containing compounds decreased post-reaction, suggesting that higher temperatures encouraged denitrogenation. Furthermore, the loss of pyrazines and increase in pyridines suggests a substitution mechanism wherein nitrogen is removed from the compound. Many of the pyrazines found in the untreated HTL-AP had short carbon chains attached to them, which could be the source of the substituted carbon.

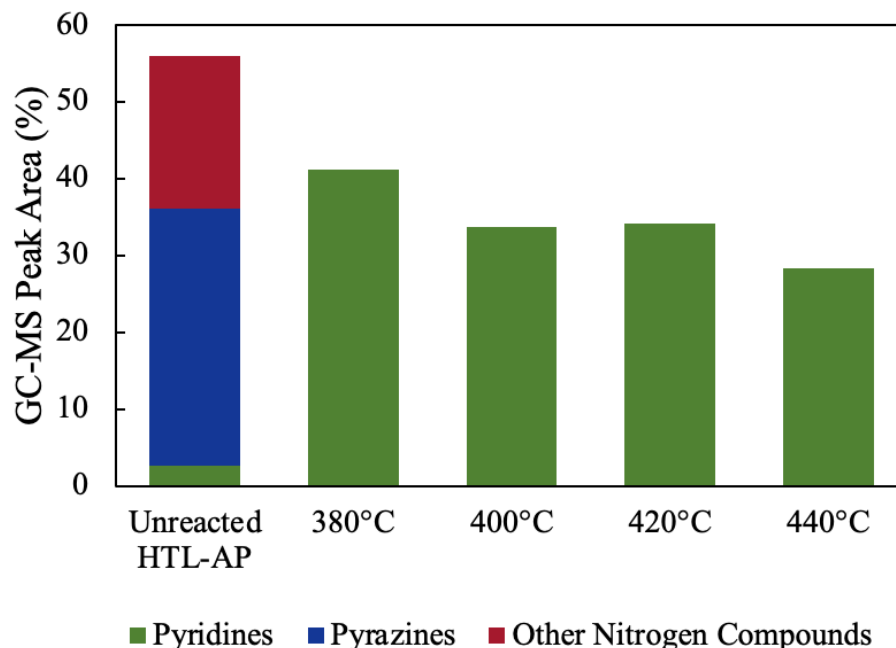


**Figure 8.** Gas chromatography and mass spectroscopy data of nitrogen-containing compounds at varying temperatures

While TOC created a curve that reaches a local minimum in TOC at 420 °C, GC/MS results indicate that activity increases with temperature until our highest trials at 440 °C. This indicates that catalyst activity continues to increase as temperature increases, but degrades almost immediately at the highest temperatures. There is thus a balance to be defined between the removal of organics and potential oil quality when operating at these conditions. Further analysis of the catalyst revealed more about this phenomenon.

### 4.3 Catalyst Stability

There were visual indicators of catalyst deactivation, such as the blackened catalyst suggesting coking on the catalyst, as pictured in Figure 9.



**Figure 9.** Photos of ZSM-5 before (left) and after (right) use in the reactor

Additionally, the decrease in yield above 420 °C suggests immediate catalyst degradation or deactivation when operating at higher temperatures. To confirm catalyst degradation, XRD analysis was performed on the spent catalyst at different operating temperatures, as shown in Figure 10.

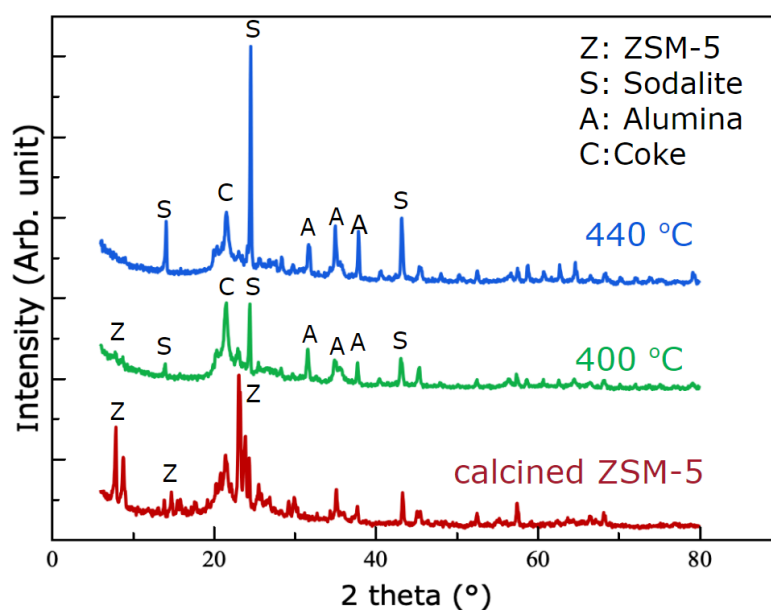


**Figure 10.** X-ray diffraction graph of ZSM-5 before and after use at different temperatures

The structure of the catalyst changed between the prepared, calcined ZSM-5 and the collected catalyst post-reaction. At higher temperatures, there is a decrease in peaks that are characteristic of ZSM-5, and instead much higher peaks for other compounds such as sodalite, alumina, and coke. At 440°C, none of the ZSM-5 peaks are left in the sample, suggesting that the ZSM-5 is completely decomposed into sodalite and alumina after 3 hours at the operating temperature of 440°C. To better understand how the catalyst degrades over time during the trials, GC/MS characterizations were analyzed of treated HTL-AP samples taken every 30 minutes over the

course of the 3-hour trials. The production of aromatics was used as an indicator of catalyst activity, a plot of which is shown in Figure 11.

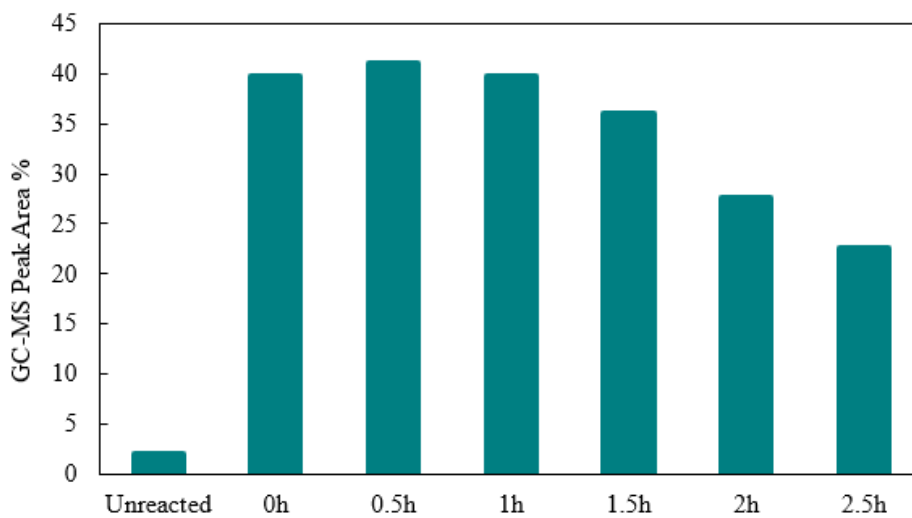


**Figure 11:** Gas chromatography and mass spectroscopy data of aromatic compounds at different times throughout a trial at 400 °C

At 400 °C, aromatics production stayed relatively constant for about 2 hours and decreased in the last hour of the trial. This indicates that the ZSM-5 is hydrothermally stable at these conditions for at least 2 hours, and the degradation seen in the XRD data only began to occur after this point. A similar trend occurred in the analysis of 380 °C trial samples, at which point the decrease in aromatics production occurred closer to 2.5 hours. It is expected that ZSM-5 will degrade faster at higher temperatures, and thus likely that degradation occurred almost immediately during the 440 °C trials. This may explain the reduction in yield that occurred at 440 °C.

#### 4.4 Techno-Economic Analysis

In order to understand the economic effect HTL-APU would have on an HTL process, a techno-economic analysis (TEA) was carried out to calculate the minimum fuel selling price (MFSP) of the bio-crude oil product and the required APU yield to offset the capital expenditures (CAPEX) related to its operation. The result of this analysis is shown in Figure 12.

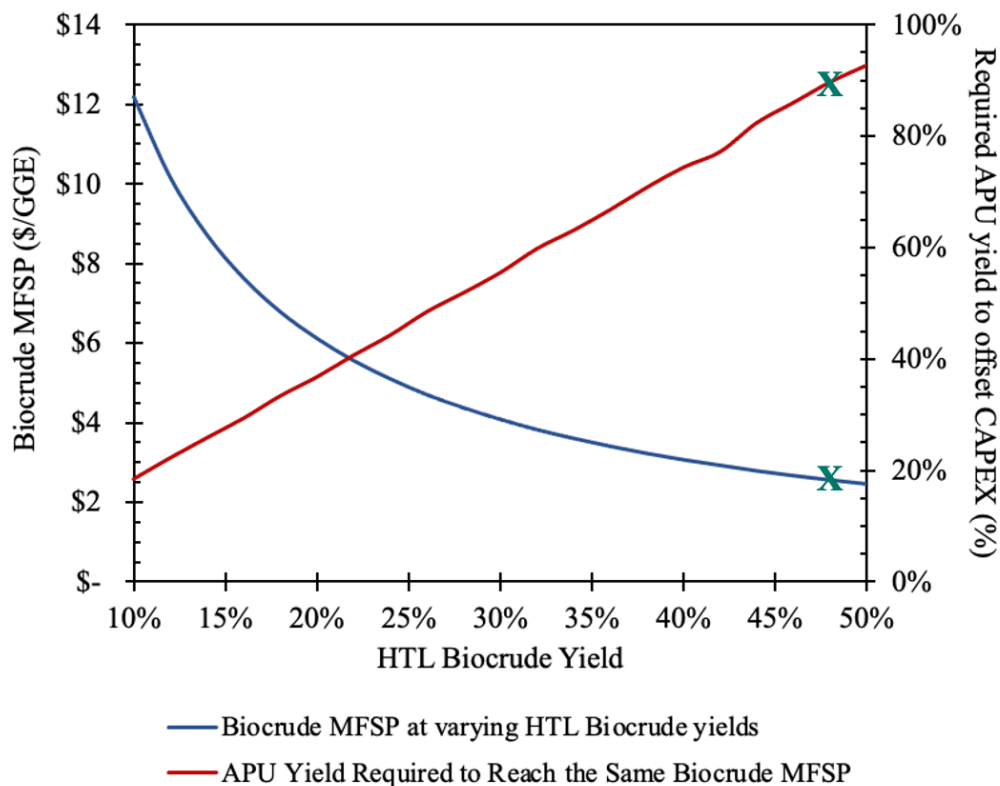


**Figure 12:** Result of the techno-economic analysis showing bio-crude selling price and the required APU yield to offset its cost

As shown in the figure above, the required APU yield increases with the bio-crude oil yield of the HTL process. At our maximum experimental APU yield of 88% (shown in green in Figure 12), the CAPEX of the APU process is offset in systems with HTL biocrude oil yields up to 47%, within the range of a typical HTL process. For this HTL operation, the cost of biocrude MFSP is estimated to be \$2.6/GGE which is relatively lower than the minimum biocrude selling price from HTL of algae of \$5-\$16/GGE (Ocampo et al., 2023).

For HTL processes with biocrude oil yields lower than 47%, the APU process adds value, driving the selling price of the bio-crude down. This allows HTL bio-crude to be more competitive with unsustainable petroleum, with the potential to become the cheaper alternative.

## 5. CONCLUSION

The removal of organics from the HTL-AP was most effective at 420 °C, at which point a local minimum of organic content occurred across all trials. The chemical activity of the catalyst continued to increase as the temperature increased, with most activity at the highest tested temperature of 440 °C. At temperatures around 440 °C and above, however, the ZSM-5 catalyst degraded almost immediately, rendering the process largely unviable. Otherwise, the ZSM-5 catalyst appeared to be hydrothermally stable at supercritical conditions for our 3-hour runs below 440 °C, with slight decreases in activity over time likely due to coking and degradation. The most effective temperature to operate this process at is thus likely closer to 420 °C. Economically, HTL-APU with our maximum yield of 88% would add value to HTL processes with bio-crude yields of less than 47%, bringing the selling price of bio-crude oil down and allowing it to compete more effectively with traditional petroleum oil.

## 6. FUTURE WORK & RECOMMENDATIONS

While these results proved that upgrading the hydrothermal liquefaction aqueous phase using ZSM-5 is a promising technique for its valorization, there are many possible improvements and research pathways to explore.

First, to improve the HTL-APU runs at the lab scale, if the reactor was redesigned to better cope with extreme temperature conditions, a more thorough study could be conducted with more trials and temperatures. This may include integrating a clam-shell design rather than the sliding block or using higher-quality piping and fittings that are better rated for the necessary conditions. The study of the temperature heating curve at the reactor could also provide a more accurate temperature set-up to meet required outlet temperature in a short time.

Second, to complete a study of the HTL-APU process for publication, a study of HTL-APU with hydrothermal-carbon stabilized ZSM-5 should be conducted to compare with ZSM-5. Research has shown that hydrothermal-carbon stabilized ZSM-5 has higher thermal stability at supercritical water conditions compared to ZSM-5 (Wang et al., 2020). Additionally, more robust characterization of the process through techniques like TN (total nitrogen) analysis could provide insight into the denitrogenation effect. The instrument used for TOC (TOC-L-CPH/CPN) can be used to detect TN with modifications to the TOC process. Similarly, installing a bubble meter for gas measuring and regenerate spent catalyst would provide a more complete carbon mass balance and understanding of the chemistry occurring throughout the process.

Lastly, to improve HTL-process at the industry scale, exploring methods to extract bio-crude or other valuable chemicals from the treated HTL-AP samples would also contribute greater value to the overall process. Organic contamination of wastewater is a large problem for many industrial processes other than HTL. Therefore, there may be potential for ZSM-5 to be applied in similar ways to treat other wastewater streams, some of which may also prove economically valuable.

## References

- Biller, P., Madsen, R. B., Klemmer, M., Becker, J., Iversen, B. B., & Glasius, M. (2016). Effect of hydrothermal liquefaction aqueous phase recycling on bio-crude yields and composition. *Bioresource Technology*, *220*, 190–199.  
<https://doi.org/10.1016/j.biortech.2016.08.053>
- Demirbas, A. (2000). Mechanisms of liquefaction and pyrolysis reactions of biomass. *Energy Conversion and Management*, *41*. [https://doi.org/10.1016/S0196-8904\(99\)00130-2](https://doi.org/10.1016/S0196-8904(99)00130-2)
- Dincer, I. (2000). Renewable energy and sustainable development: A crucial review. *Renewable and Sustainable Energy Reviews*, *4*(2), 157–175.  
[https://doi.org/10.1016/S1364-0321\(99\)00011-8](https://doi.org/10.1016/S1364-0321(99)00011-8)
- Duan, P., Bai, X., Xu, Y., Zhang, A., Wang, F., Zhang, L., & Miao, J. (2013). Catalytic upgrading of crude algal oil using platinum/gamma alumina in supercritical water. *Fuel*, *109*, 225–233. <https://doi.org/10.1016/j.fuel.2012.12.074>
- Gollakota, A. R. K., Kishore, N., & Gu, S. (2018). A review on hydrothermal liquefaction of biomass. *Renewable and Sustainable Energy Reviews*, *81*, 1378–1392.  
<https://doi.org/10.1016/j.rser.2017.05.178>
- Han, Y., Liu, C., Horita, J., & Yan, W. (2016). Trichloroethene hydrodechlorination by Pd-Fe bimetallic nanoparticles: Solute-induced catalyst deactivation analyzed by carbon isotope fractionation. *Applied Catalysis B: Environmental*, *188*, 77–86.  
<https://doi.org/10.1016/j.apcatb.2016.01.047>
- Ji, Y., Yang, H., & Yan, W. (2017). Strategies to enhance the catalytic performance of ZSM-5 zeolite in hydrocarbon cracking: A review. *Catalysts*, *7*(12), Article 12.

<https://doi.org/10.3390/catal7120367>

Kariim, I., Swai, H., & Kivevele, T. (2023). Bio-oil upgrading over ZSM-5 catalyst: A review of catalyst performance and deactivation. *International Journal of Energy Research*, 2023, e4776962. <https://doi.org/10.1155/2023/4776962>

Kulikova, Y., Klementev, S., Sirotkin, A., Mokrushin, I., Bassyouni, M., Elhenawy, Y., El-Hadek, M. A., & Babich, O. (2023). Aqueous phase from hydrothermal liquefaction: Composition and toxicity assessment. *Water*, 15(9), Article 9. <https://doi.org/10.3390/w15091681>

LeClerc, H. O., Page, J. R., Tompsett, G. A., Niles, S. F., McKenna, A. M., Valla, J. A., Timko, M. T., & Teixeira, A. R. (2023). Emergent chemical behavior in mixed food and lignocellulosic green waste hydrothermal liquefaction. *ACS Sustainable Chemistry & Engineering*, 11(6), 2427–2439. <https://doi.org/10.1021/acssuschemeng.2c06266>

Li, X., Zhang, L., Wang, S., & Wu, Y. (2020). Recent advances in aqueous-phase catalytic conversions of biomass platform chemicals over heterogeneous catalysts. *Frontiers in Chemistry*, 7. <https://www.frontiersin.org/articles/10.3389/fchem.2019.00948>

Li, Z., & Savage, P. E. (2013). Feedstocks for fuels and chemicals from algae: Treatment of crude bio-oil over HZSM-5. *Algal Research*, 2(2), 154–163. <https://doi.org/10.1016/j.algal.2013.01.003>

Maag, A. R., Tompsett, G. A., Tam, J., Aik Ang, C., Azimi, G., D. Carl, A., Huang, X., J. Smith, L., L. Grimm, R., Q. Bond, J., & T. Timko, M. (2019). ZSM-5 decrystallization and dealumination in hot liquid water. *Physical Chemistry Chemical Physics*, 21(32), 17880–17892. <https://doi.org/10.1039/C9CP01490J>

McKendry, P. (2002). Energy production from biomass (part 1): Overview of biomass.

- Bioresource Technology*, 83(1), 37–46. [https://doi.org/10.1016/S0960-8524\(01\)00118-3](https://doi.org/10.1016/S0960-8524(01)00118-3)
- Ocampo, E., Beltrán, V. V., Gómez, E. A., Ríos, L. A., & Ocampo, D. (2023). Hydrothermal liquefaction process: Review and trends. *Current Research in Green and Sustainable Chemistry*, 7, 100382. <https://doi.org/10.1016/j.crgsc.2023.100382>
- Onyanta, A. (2016). Cities, municipal solid waste management, and climate change: Perspectives from the South. *Geography Compass*, 10(12), 499–513. <https://doi.org/10.1111/gec3.12299>
- Ramirez, J. A., Brown, R. J., & Rainey, T. J. (2015). A review of hydrothermal liquefaction bio-crude properties and prospects for upgrading to transportation fuels. *Energies*, 8(7), Article 7. <https://doi.org/10.3390/en8076765>
- Snowden-Swan, L. J., Zhu, Y., Jones, S. B., Elliott, D. C., Schmidt, A. J., Hallen, R. T., Billing, J. M., Hart, T. R., Fox, S. P., & Maupin, G. D. (2016). *Hydrothermal liquefaction and upgrading of municipal wastewater treatment plant sludge: A preliminary techno-economic analysis* (PNNL--25464, 1258731; p. PNNL--25464, 1258731). <https://doi.org/10.2172/1258731>
- SundarRajan, P., Gopinath, K. P., Arun, J., GracePavithra, K., Adithya Joseph, A., & Manasa, S. (2021). Insights into valuing the aqueous phase derived from hydrothermal liquefaction. *Renewable and Sustainable Energy Reviews*, 144, 111019. <https://doi.org/10.1016/j.rser.2021.111019>
- Swetha, A., ShriVigneshwar, S., Gopinath, K. P., Sivaramakrishnan, R., Shanmuganathan, R., & Arun, J. (2021, November). *Review on hydrothermal liquefaction aqueous phase as a valuable resource for biofuels, bio-hydrogen and valuable bio-chemicals recovery*. ScienceDirect.

- <https://www.sciencedirect.com/science/article/pii/S0045653521017203?via%3Dihub>
- Tian, K., Liu, W.-J., Qian, T., Jiang, H., & Yu, H.-Q. (2014). Investigation on the evolution of N-containing organic compounds during pyrolysis of sewage sludge. *Environmental Science & Technology*, 48. <https://doi.org/10.1021/es5022137>
- Toor, S. S., Rosendahl, L., & Rudolf, A. (2011). Hydrothermal liquefaction of biomass: A review of subcritical water technologies. *Energy*, 36(5), 2328–2342. <https://doi.org/10.1016/j.energy.2011.03.013>
- Valdez, P. J., Nelson, M. C., Wang, H. Y., Lin, X. N., & Savage, P. E. (2012). Hydrothermal liquefaction of *Nannochloropsis* sp.: Systematic study of process variables and analysis of the product fractions. *Biomass and Bioenergy*, 46, 317–331. <https://doi.org/10.1016/j.biombioe.2012.08.009>
- Wang, Y., Guerra, P., Zaker, A., Maag, A. R., Tompsett, G. A., Smith, L. J., Huang, X., Bond, J. Q., & Timko, M. T. (2020). Strategies for extending zeolite stability in supercritical water using thermally stable coatings. *ACS Catalysis*, 10(12), 6623–6634. <https://doi.org/10.1021/acscatal.0c01722>
- Watson, J., Wang, T., Si, B., Chen, W.-T., Aierzhati, A., & Zhang, Y. (2020). Valorization of hydrothermal liquefaction aqueous phase: Pathways towards commercial viability. *Progress in Energy and Combustion Science*, 77, 100819. <https://doi.org/10.1016/j.pecs.2019.100819>
- Wu, K., Gao, Y., Zhu, G., Zhu, J., Yuan, Q., Chen, Y., Cai, M., & Feng, L. (2017). Characterization of dairy manure hydrochar and aqueous phase products generated by hydrothermal carbonization at different temperatures. *Journal of Analytical and Applied Pyrolysis*, 127, 335–342. <https://doi.org/10.1016/j.jaap.2017.07.017>

- Wu, K., Wu, Y., Chen, Y., Chen, H., Wang, J., & Yang, M. (2016). Heterogeneous catalytic conversion of biobased chemicals into liquid fuels in the aqueous phase. *ChemSusChem*, 9(12), 1355–1385. <https://doi.org/10.1002/cssc.201600013>
- Zaker, A., Tompsett, G. A., Wang, S., Bond, J. Q., & Timko, M. T. (2022). Supercritical water promoted aromatics production using ZSM-5 catalyst. *Fuel*, 310, 122360. <https://doi.org/10.1016/j.fuel.2021.122360>

# Appendices

## Appendix A: Instructions of Characterization Techniques

### Appendix A.1: Instruction of sample preparation for total organic content analysis (TOC)

TOC analyses were carried out with a Shimadzu Co. TOC-L Series Analyser. To perform this analysis, samples were diluted to a dilution factor of  $1.5 \times 10^{-4}$ . This was accomplished by diluting 15  $\mu\text{g}$  of sample in 100 mL of reagent-grade water.

Procedure to prepare stocks and stock standards

- 1) Prepare a stock 1000 ppm OC standard solution by measuring 0.5314 g of Potassium Hydrogen Phthalate (KHP) into a 250 mL volumetric flask filled to the mark with reagent-grade water.
- 2) Dilute the stock standard into three standard solutions with concentrations of 10, 6, and 2 mg/L, with a fourth standard of pure water.

Procedure to prepare collected samples

- 1) Prepare samples by filling 100 mL volumetric flasks about halfway with water, adding 1 mL of a 6N HCl solution, adding 15  $\mu\text{g}$  of the desired sample using a volumetric pipette, and filling the flask up with water to the 100 mL mark.
- 2) Repeat the procedures for all required samples.

### Appendix A.2: Instruction of sample preparation for Gas Chromatography-Mass Spectrometry (GC-MS)

Procedure to prepare 1:1 DCM Extraction Samples. For safety protocols, the preparation should be conducted in the fume hood.

- 1) Mix 2 mL of treated HTL-AP samples with 2 mL of dichloromethane (DCM)
- 2) Shake the sample for 30 seconds and leave the sample to separate the layer for 30 minutes
- 3) Extract 1 mL of the DCM phase (the bottom layer) into a vial for further GC/MS injection.

## Appendix B: HTL-AP and Catalyst Characterization

### Appendix B.1: Raman Spectroscopy Analysis of Catalyst Pre and Post-Calcination

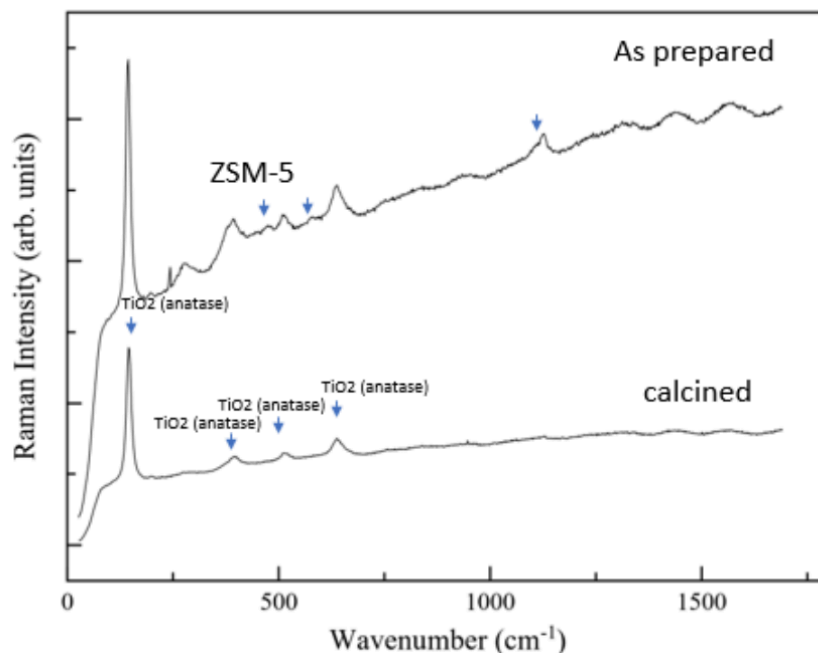


**Figure 13.** Raman Spectroscopy analysis of ZSM-5 as prepared and calcined ZSM-5

Only  $\text{TiO}_2$  or anatase phase of ZSM-5 appears on catalyst pre and post calcination, suggesting no change in catalyst composition.

### Appendix B.2: Interpretation of GC-MS Analysis—Compound Groups Selection

The GC/MS returned a data sheet with a table of compounds and their respective peak areas and area percents, an example of which is shown below:

Peak#	Ret.Time	Proc.From	Proc.To	Mass	Area	Height	A/H	Conc.	Mark	Name	Ret. Index
1	4.13	4.11	4.19	TIC	37639	12421	3.03	0.24		2-Butanol, 3-methyl-	
2	4.211	4.19	4.355	TIC	1615684	675455	2.39	10.37	SV	2-Pentanone	
3	4.345	4.335	4.355	TIC	751	3395	0.22		T	Ether, chloromethyl dichloromethyl	
4	4.404	4.38	4.515	TIC	714917	278133	2.57	4.59		3-Pentanone	
5	4.69	4.655	4.715	TIC	22458	10690	2.1	0.14		2-Butanone, 3,3-dimethyl-	
6	5.373	5.34	5.41	TIC	61290	31497	1.95	0.39		Methyl Isobutyl Ketone	
7	5.455	5.41	5.595	TIC	854077	264856	3.22	5.48	V	Pyridine	
8	5.642	5.595	5.66	TIC	129361	51405	2.52	0.83	V	3-Pentanone, 2-methyl-	
9	5.684	5.66	5.775	TIC	197073	60990	3.23	1.27	V	2-Pentanone, 3-methyl-	
10	6.034	5.99	6.105	TIC	98396	36083	2.73	0.63		Toluene	
11	6.567	6.535	6.665	TIC	142476	47017	3.03	0.91		3-Hexanone	
12	6.714	6.665	6.83	TIC	362987	103862	3.49	2.33	V	Cyclopentanone	
13	7.347	7.33	7.41	TIC	55908	20457	2.73	0.36		3,5-Dihydroxycyclohexanamine	
14	7.433	7.41	7.585	TIC	971628	308318	3.15	6.24		Pyridine, 2-methyl-	
15	8.276	8.24	8.325	TIC	41787	16698	2.5	0.27		Cyclohexanone	
16	8.474	8.435	8.565	TIC	113503	31461	3.61	0.73		(R)-(+)-3-Methylcyclopentanone	
17	8.665	8.65	8.71	TIC	25459	15962	1.59	0.16		2H-Pyran-2,4(3H)-dione, dihydro-6-methyl-	
18	8.882	8.865	9.055	TIC	727814	179118	4.06	4.67		Pyridine, 3-methyl-	
19	9.193	9.135	9.265	TIC	170380	49604	3.43	1.09		Benzene, 1,3-dimethyl-	
20	9.605	9.59	9.63	TIC	6698	4791	1.4	0.04		Acetamide, 2,2,2-trifluoro-N-(1-methylpiperidin-4-yl)-	
21	9.651	9.63	9.77	TIC	432709	136044	3.18	2.78	V	Pyridine, 2,6-dimethyl-	
22	9.996	9.945	10.045	TIC	90459	30386	2.98	0.58		o-Xylene	
23	10.22	10.195	10.25	TIC	20097	12260	1.64	0.13		2-Pentanone, 3-methyl-	

**Figure 14:** Example of raw GC/MS data

Because of this, the SUMIF excel function was used to group these compounds together to analyse trends in our data. An example of the use of this function is shown below:

=SUMIF('400C\_0h'!\$K:\$K,'\*Pyrazine\*',400C\_0h'!\$I:\$I)

Where the referenced sheet contains a list of compound names in column K and their respective area percents in column I. This returns a sum of all compounds in the sample that contain pyrazine. This was repeated for all samples for many different compounds, resulting in a table of compounds like the one shown below:

	Pyridine		Pentanones		Aromatics											
	*Pyrazine*	*Pyridine*	*-Pentanone*	*Cyclopen*	*p-Cresol*	*Benzaldehyde*	*phenol*	*Toluene*	*furan*	*phenylethyl alcohol*	*Quinoline*	SUM				
5	Unreacted	30	2.58	1.95	28.74	1.16	0	0	0	0.73	0	1.89				
6	UNR-CF	33.57	1.17	0.64	29.51	0.62	0	2.34	0	0.66	0	3.62				
7	400C 0h	0.00	32.88	20.06	3.78	0.00	0.00	33.47	0.00	0.00	0.00	33.47				
8	400C 2.5h	2.02	28.5	15.76	14.82	0	0	20.46	0	0	0	20.46				
9	380C 0h 2	0	35.17	20.86	2.63	0	0	26.24	0.82	0	0	27.06				
10	380C 2.5h 2	9.51	18.65	12.28	24.08	0	0	17.91	1.21	0.01	0	19.12				
11	380C 0h 3	0	47.35	11.31	7.87	0	0	27.47	1.37	0.02	0	28.84				
12	380C .5h 3	1.87	42.98	11	20.52	0	0	37.04	2.86	0	0	39.90				
13	380C 1h 3	0	28.87	20.74	9.14	0	0	33.69	0.85	0	0	34.54				
14	380C 1.5h 3	0	31.03	19.3	10.08	0	0	31.15	0	0	0	31.15				
15	380C 2h 3	0.34	32.69	17.67	8.78	0	0	29.66	0.94	0	0	30.60				
16	380C 2.5h 3	1.67	32.09	17.19	13.43	0	0	26.34	0.63	0	0	26.97				
17	400C 0h 4	0.05	34.67	20.3	1.43	0	0	32.2	1.02	0	0	33.22				
18	400C .5h 4	0	25.83	24.48	2.12	0	0	36.8	0	0	0	36.8				
19	400C 1h 4	0	31.53	20.64	2.07	0	0	35.4	0.87	0	0	36.27				
20	400C 1.5h 4	0	34.54	19.56	4.42	0	0	31.69	0	0.01	0	31.70				
21	400C 2h 4	0.3	35.8	19.11	11.04	0	0.03	24.04	0.68	0	0	24.71				
22	400C 2.5h 4	3.99	30.61	14.81	23.33	0	0	20.2	0.34	0	0	20.54				
23	420C 0h 5	0	34.2	14.59	0	0	0	46.03	0	0	0	46.03				
24	420C 2.5h 5	33.66	10	9.52	16.97	0	0	18.95	0	0	0	18.95				
25	440C 0h 7	0	28.36	16.18	0	0	0	48.35	0.78	0	0	49.13				
26	440C 2.5h 7	11.46	24.15	12.85	17.58	0	0	28.14	0.2	0.08	0	28.42				

Figure 15: Table created by using the SUMIF function to analyze GC/MS data

This data was then used to create the charts shown in section 4.

### Appendix C: HTL-APU Yield Calculation

Example calculation of HTL-APU Yield at the operating temperature of 380 °C

TOC of pre-treated HTL-AP = 17973.3 PPM

TOC of HTL-AP after 3 hours of HTL-AP at 380 °C = 5634.7 PPM

$$\text{HTL-APU Yield} = \frac{17973.3 - 5634.7}{17973.3} = 68.65 \approx 69\%$$

## Appendix D: Experimental Data

### Appendix D.1: Important Experimental Parameters Observed During HTL-APU Runs

**Table 2.** Experimental Data from HTL-APU run at 380 °C

Time (h)	Trial #1				Trial #2			
	Tout (°C)	Pin (PSI)	Pout (PSI)	Mass of HTL-AP (g)	Tout (°C)	Pin (PSI)	Pout (PSI)	Mass of HTL-AP (g)
0	384	3650	3500	-	382	3670	3500	-
0.5	383	3650	3500	-	383	3670	3500	-
1	382	3650	3500	-	383	3670	3500	-
1.5	386	3650	3500	-	384	3670	3500	-
2	383	3650	3500	-	387	3670	3500	-
2.5	382	3650	3500	-	391	3670	3500	-

**Table 3.** Experimental Data from HTL-APU run at 400 °C

Time (h)	Trial #1				Trial #2			
	Tout (°C)	Pin (PSI)	Pout (PSI)	Mass of HTL-AP (g)	Tout (°C)	Pin (PSI)	Pout (PSI)	Mass of HTL-AP (g)
0	407	3670	3500	-	404	3500	3300	8.4
0.5	404	3870	3500	-	406	3500	3300	7.53
1	410	3800	3500	-	400	3600	3300	7.42
1.5	413	3860	3500	-	407	3650	3300	7.18
2	400	3600	3500	-	410	3600	3300	-
2.5	407	4550	3500	-	413	3650	3300	-

**Table 4.** Experimental Data from HTL-APU run at 420 °C

Time (h)	Trial #1				Trial #2			
	Tout (°C)	Pin (PSI)	Pout (PSI)	Mass of HTL-AP (g)	Tout (°C)	Pin (PSI)	Pout (PSI)	Mass of HTL-AP (g)
0	425	3640	3500	7.77	425	3700	3500	9.62
0.5	424	3650	3500	7.8	418	3600	3450	3.13
1	423	3650	3500	7.68	420	3600	3450	9.06
1.5	416	3650	3500	7.59	410	3600	3450	7.27
2	415	3650	3500	7.91	421	3650	3500	6.16
2.5	422	3650	3500	7.76	425	3650	3500	6.09

**Table 5.** Experimental Data from HTL-APU run at 440 °C

Time (h)	Trial #1				Trial #2			
	Tout (°C)	Pin (PSI)	Pout (PSI)	Mass of HTL-AP (g)	Tout (°C)	Pin (PSI)	Pout (PSI)	Mass of HTL-AP (g)
0	435	3600	3450	8.12	440	3800	3500	7.58
0.5	430	3600	3450	7.18	437	4600	3500	6.72
1	450	3650	3450	7.12	446	4000	3500	7.16
1.5	442	3650	3450	7.87	450	4500	3500	6.2
2	448	3650	3450	8.27	460	3850	3500	7.01
2.5	445	3630	3450	6.53	440	4300	3500	-

## Appendix D.2: Example of GC-MS Results

C Peak Table]

# of Peaks 47

Peak#	Ret.Time	Proc.Fron	Proc.To	Mass	Area	Height	A/H	Conc.	Mark	Name	Ret. Index
1	4.029	4.01	4.06	TIC	16910	8933	1.89	0.16		Butanenitrile	
2	4.135	4.06	4.19	TIC	20973	8240	2.55	0.2	V	2-Pentanol	
3	4.211	4.19	4.36	TIC	1313921	558249	2.35	12.52		2-Pentanone	
4	4.406	4.38	4.505	TIC	494862	200976	2.46	4.72		3-Pentanone	
5	4.96	4.91	5.03	TIC	77245	23586	3.28	0.74		Chloriodomethane	
6	5.377	5.355	5.425	TIC	39255	21420	1.83	0.37		Methyl Isobutyl Ketone	
7	5.466	5.425	5.605	TIC	672678	210406	3.2	6.41	V	Pyridine	
8	5.649	5.605	5.66	TIC	78983	34940	2.26	0.75	V	3-Pentanone, 2-methyl-	
9	5.69	5.66	5.775	TIC	137318	42222	3.25	1.31	V	2-Pentanone, 3-methyl-	
10	6.576	6.545	6.64	TIC	64562	26389	2.45	0.62		3-Hexanone	
11	6.727	6.64	6.81	TIC	152791	44803	3.41	1.46	V	N-(n-Butoxymethyl)acrylamide	
12	7.36	7.345	7.43	TIC	42813	17096	2.5	0.41		3,5-Dihydroxycyclohexanamine	
13	7.443	7.43	7.66	TIC	828971	227753	3.64	7.9	S	Pyridine, 2-methyl-	
14	7.615	7.61	7.625	TIC	409	2840	0.14	0	T	Carbamic acid, N-(3-nitropyrid-4-yl)-, ethyl ester	
15	8.492	8.46	8.515	TIC	18646	9879	1.89	0.18		Cyclopentanone, 3-methyl-	
16	8.897	8.88	9.04	TIC	468074	119875	3.9	4.46		Pyridine, 3-methyl-	
17	9.667	9.635	9.79	TIC	250397	76007	3.29	2.39		Pyridine, 2,6-dimethyl-	
18	10.393	10.365	10.46	TIC	165490	55294	2.99	1.58		Pyridine, 2-ethyl-	
19	10.503	10.46	10.59	TIC	120392	32615	3.69	1.15	V	2-Cyclopenten-1-one, 2-methyl-	
20	11.228	11.19	11.355	TIC	353599	85096	4.16	3.37		Pyridine, 2,5-dimethyl-	
21	11.739	11.715	11.81	TIC	92151	30821	2.99	0.88		Pyridine, 2,3-dimethyl-	
22	12.222	12.195	12.255	TIC	46629	20874	2.23	0.44		Pyridine, 3-ethyl-	
23	12.468	12.425	12.53	TIC	85215	31838	2.68	0.81		Pyridine, 2-ethyl-6-methyl-	
24	13.242	13.165	13.345	TIC	954879	234331	4.07	9.1		Phenol	
25	13.443	13.345	13.525	TIC	98187	42221	2.33	0.94	V	Pyridine, 2,4,6-trimethyl-	
26	13.77	13.75	13.785	TIC	8930	5179	1.72	0.09		Pyrimidine-2, 4(1H, 3H)-dione, 5-iodo-1-(N-methyl-N-methylsulfonyl)aminomethyl-	
27	13.805	13.785	13.91	TIC	78025	14597	5.35	0.74	V	Pyridine, 3,5-dimethyl-	
28	14.515	14.485	14.545	TIC	15084	8920	1.69	0.14		Pyridine, 2-ethyl-5-methyl-	
29	15.034	14.96	15.15	TIC	749218	197454	3.79	7.14		2-Cyclopenten-1-one, 2,3-dimethyl-	
30	15.674	15.6	15.75	TIC	551794	151079	3.65	5.26		Phenol, 2-methyl-	
31	15.854	15.75	15.93	TIC	168790	45353	3.72	1.61	V	2-Cyclopenten-1-one, 3,4,4-trimethyl-	
32	16.025	15.985	16.075	TIC	41673	16992	2.45	0.4		2-Ethyl-3,5-dimethylpyridine	
33	16.243	16.195	16.275	TIC	30277	9423	3.21	0.29		o-Toluidine	
34	16.371	16.275	16.485	TIC	805153	185936	4.33	7.67	V	Phenol, 3-methyl-	
35	16.615	16.565	16.695	TIC	59988	16770	3.58	0.57		Pyridine, 4-ethyl-2,6-dimethyl-	
36	16.756	16.7	16.83	TIC	101972	28727	3.55	0.97		Ethanone, 1-(1-cyclohexen-1-yl)-	
37	17.217	17.14	17.275	TIC	98852	20174	4.9	0.94		Cyclohexanone, 3-ethenyl-	
38	17.346	17.275	17.39	TIC	31528	10894	2.89	0.3	V	Phenol, 2,6-dimethyl-	
39	18.136	18.095	18.21	TIC	87250	25632	3.4	0.83		Cyclohexanone, 3-ethenyl-	
40	18.384	18.335	18.465	TIC	184026	50691	3.63	1.75		Phenol, 2-ethyl-	
41	18.733	18.635	18.8	TIC	208840	47463	4.4	1.99		Phenol, 2,5-dimethyl-	
42	19.35	19.23	19.445	TIC	462587	98235	4.71	4.41		Phenol, 3-ethyl-	
43	19.641	19.595	19.715	TIC	70483	20665	3.41	0.67		Phenol, 2,6-dimethyl-	
44	21.465	21.44	21.505	TIC	18464	6213	2.97	0.18		1,3-Cyclohexadiene, 1,5,5,6-tetramethyl-	
45	21.543	21.505	21.585	TIC	40693	13904	2.93	0.39	V	Quinoline	
46	23.623	23.575	23.675	TIC	56633	16847	3.36	0.54		Isoquinoline, 1-methyl-	
47	23.759	23.705	23.8	TIC	26477	8758	3.02	0.25		Cyclohexasiloxane, dodecamethyl-	

**Figure 16.** Screenshot of compounds name and peak areas, obtained from GC/MS) in treated HTL-AP at 380 °C & 1.5h

### Appendix D.3: Example of TOC Results

The TOC result returned by the Shimadzu machine contained a list of results for each sample, all with the following format:

#### Sample

Sample Name: 2024\_03\_25\_APU\_MQP\_Run3  
 Sample ID: Used, prepped 3/25  
 Origin: DK NPOC 10ppm.met  
 Status: Completed  
 Chk. Result

Type	Anal.	Manual Dilution	Result
Unknown	NPOC	1.000	NPOC:0.6854mg/L

1. Det

Anal.: NPOC

No.	Area	Conc.	Inj. Vol.	Aut. Dil.	Ex.	Cal. Curve	Date / Time
1	5.032	0.7377mg/L	50ul	1.000		DK NPOC 10ppm.2024_03_26_07_06_59.cal	3/26/2024 9:13:08 AM
2	4.710	0.6415mg/L	50ul	1.000		DK NPOC 10ppm.2024_03_26_07_06_59.cal	3/26/2024 9:15:56 AM
3	4.829	0.6771mg/L	50ul	1.000		DK NPOC 10ppm.2024_03_26_07_06_59.cal	3/26/2024 9:18:41 AM
4	4.286	0.5148mg/L	50ul	1.000	E	DK NPOC 10ppm.2024_03_26_07_06_59.cal	3/26/2024 9:21:11 AM
5	4.426	0.5566mg/L	50ul	1.000	E	DK NPOC 10ppm.2024_03_26_07_06_59.cal	3/26/2024 9:23:56 AM

Mean Area 4.857  
 Mean Conc. 0.6854mg/L  
 SD Area 0.1628  
 CV Area 3.35%

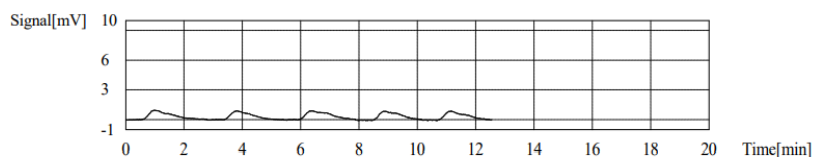


**Figure 17:** Example of TOC return sheet

The TOC analyser returned an NPOC number for each sample in mg/L, which was then multiplied by the dilution factor to obtain the actual TOC of the sample.